



Tyrphostin-like compounds with ubiquitin modulatory activity as possible therapeutic agents for multiple myeloma

Zhenghong Peng^a, Ashutosh Pal^b, Dongmei Han^{a,b,c,d}, Shimei Wang^{a,b,c,d}, David Maxwell^a, Alexander Levitzki^c, Moshe Talpaz^d, Nicholas J. Donato^d, William Bornmann^{a,*}

^a Department of Experimental Therapeutics, M. D. Anderson Cancer Center, Houston, TX 77030, United States

^b Experimental Diagnostic Imaging Chemistry Section, M. D. Anderson Cancer Center, Houston, TX 77030, United States

^c Unit of Cellular Signaling, Department of Biological Chemistry, The Hebrew University of Jerusalem, Jerusalem, Israel

^d Department of Internal Medicine/Division of Hematology/Oncology, University of Michigan Comprehensive Cancer Center, Ann Arbor, MI 48109, United States

ARTICLE INFO

Article history:

Received 20 April 2011

Revised 22 September 2011

Accepted 28 September 2011

Available online 7 October 2011

Keywords:

Tyrphostin analogs

Multiple myeloma

Jak2/Stat3

Small molecules

Inhibitors

Synthesis

Quantum chemical calculations

ABSTRACT

With the goal of developing small molecules as novel regulators of signal transduction and apoptosis, a series of tyrphostin-like compounds were synthesized and screened for their activity against MM-1 (multiple myeloma) cells and other cell lines representing this malignancy. Synthesis was completed in solution-phase initially and then adopted to solid-phase for generating a more diverse set of compounds. A positive correlation was noted between compounds capable of inducing apoptosis and their modulation of protein ubiquitination. Further analysis suggested that ubiquitin modulation occurs through inhibition of cellular deubiquitinase activity. Bulky groups on the sidechain near the α,β -unsaturated ketone caused a complete loss of activity, whereas cyclization on the opposite side was tolerated. Theoretical calculations at the B3LYP/LACV3P** level were completed on each molecule, and the resulting molecular orbitals and Fukui reactivity values for C_β carbon were utilized in developing a model to explain the compound activity.

© 2011 Elsevier Ltd. All rights reserved.

1. Introduction

Signaling proteins are key components of the cellular circuitry that link internal and external stimuli to changes in cell morphology and gene expression and are highly regulated in normal cells. In pathologies, including cancer, regulation of signaling proteins is disrupted by gene mutations and chromosomal translocations resulting in unregulated growth and survival, tumor metastases and blocked differentiation. Reducing expression or returning signaling proteins to their inactive state reverses many of the characteristics associated with cancer and these proteins serve as effective targets for cancer and other therapies.

AG490 (Fig. 1) was the first small molecule found to inhibit Jak2/Stat3 signaling.¹ Targeted inhibition of the Jak/Stat pathway with **AG490** inhibits tumor cell growth and increases sensitivity to apoptotic stimuli; thus, inhibitors of this pathway represent potential therapeutics for cancer and possibly other diseases.^{2–4} Because the cytokine IL-6 promotes survival and proliferation of certain cancerous cell lines through the phosphorylation of STAT3,^{5–7} kinase inhibitors similar to **AG490** have potential as anti-cancer drugs. Compound **AG490** is structurally classified as a tyrphostin. US Patent

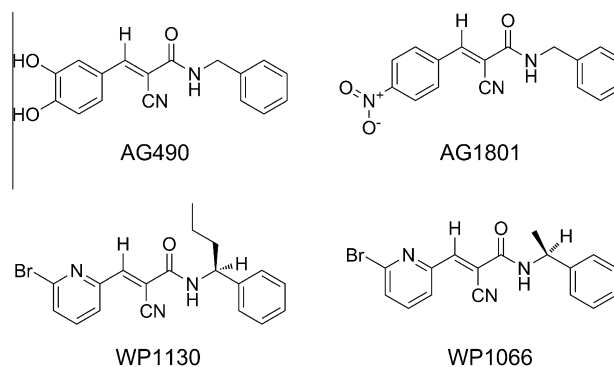


Figure 1. Chemical structures of several commonly named tyrphostins discussed in paper.

WO9528922,⁸ WO2003068157,⁹ and WO2005058829¹⁰ describe compounds that have structural similarity with **AG490**. Unfortunately, **AG490** has limited activity in animal studies due to pharmacokinetic properties and must be used at high concentrations (~50 to 100 μ M). Also, it is difficult to always document the ability of **AG490** to inhibit Jak2/Stat3 signaling in vivo.^{1,11,12} We therefore sought to modify **AG490** in order to achieve more drug-like

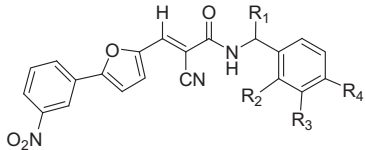
* Corresponding author. Tel.: +1 713 563 0081; fax: +1 713 563 1878.

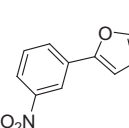
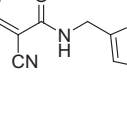
E-mail address: wbornmann@mdanderson.org (W. Bornmann).

Table 1a
Anti-tumor activity of compounds against multiple myeloma cell lines

Compd	X	R ₁	R ₂	R ₃	R ₄	R ₅	R ₆	R ₇	R ₈	R ₉	IC ₅₀ μM		
											MM-1	U266	OCI-My4
AG490	CH	OH	OH	H	H	H	H	H	H	H	>10	>12.5	>12.5
AG1801	CH	H	NO ₂	H	H	H	H	H	H	H	7.5	9.0	12.0
WP1130	N	Br	H	H	H	nPr	H	H	H	H	1.0	1.3	1.5
WP1066	N	Br	H	H	H	Me	H	H	H	H	1.2	1.5	1.8
5	N	Br	H	H	H	Me	H	H	Br	H	1.5	1.8	2.0
6	N	Br	H	H	H	Me	H	H	OMe	H	1.2	1.4	1.8
7	N										2	2.5	ND
8	N										1.5	1.9	ND
9	N	Br	H	H	H	Me	H	H	Cl	H	1.6	2.0	2.3
10	N	Br	H	H	H	CH ₂ OH	H	H	H	H	2.8	3.5	3.9
11	N	Br	H	H	H	Et	H	H	H	H	1.1	1.4	1.7
12	N	Br	H	H	H	Me	H	H	H	OMe	2.4	2.8	3.1
13	N	Br	H	H	H	Me	H	H	Cl	H	2.1	2.3	2.4
14	N	Br	H	H	H	CF ₃	H	H	H	H	9.6	11.1	ND
15	N	Br	H	H	H	Me	H	CF ₃	H	H	1.3	1.6	1.8
16	N	Br	H	H	H	Me	H	H	F	H	1.2	1.4	ND
17	N	Br	H	H	H	Me	H	CF ₃	H	CF ₃	1.3	1.5	ND
18	N	Br	H	H	H	CH ₂ COOCH ₃	H	H	H	H	3.1	3.3	ND
19	N	Br	H	H	H	Me	F	H	H	H	1.8	2.0	2.4
20	N	Br	H	H	H		H	H	H	H	1.1	1.3	1.6
21	CH	NO ₂	Cl	H	H		H	H	H	H	2.5	2.8	2.9
22	CH	H		H	H		H	H	H	H	>10	>10	ND
23	N	Br	H	H	H		H	H	H	H	1.4	ND	ND
24	CH	H	Hexanyl-	H	H		H	H	H	H	>10	ND	ND
25	N	Br	H	H	H	Me	H	H	NH ₂	H	>10	ND	ND
26	N	Br	H	H	H	H	H	NH ₂	H	H	>10	ND	ND
27	CH	H	NO ₂	H	H	nPr	H	H	H	H	2.94	3.6	ND
28	C-NO ₂	H	NO ₂	H	H	nPr	H	H	H	H	>10	ND	ND
29	CH	H	H	H	H	nPr	H	H	H	H	6.25	7.2	ND
30	CH	NO ₂	H	H	H	nPr	H	H	H	H	1.73	2.1	2.2
31	CH	H	Cl	NO ₂	H	nPr	H	H	H	H	1.58	1.8	1.9
32	C-NO ₂	H	H	H	Cl	nPr	H	H	H	H	>10	ND	ND
33	CH	H	OH	H	H	nPr	H	H	H	H	>10	ND	ND
34	CH	NO ₂	OH	H	H	nPr	H	H	H	H	8.2	9.3	9.7
35	CH	Br	OH	H	H	nPr	H	H	H	H	>10	ND	ND
36	N	Br	H	H	H	CH ₂ OCOCH ₃	H	H	H	H	2.6	2.8	2.9
37	CH	NO ₂	NO ₂	H	H	Me	H	H	H	H	>10	ND	ND
38	N	Br	H	H	H	Ph	H	H	H	H	5	5.8	6.2
39	N	Br	H	H	H	Bn	H	H	H	H	2.5	2.7	2.9
40	CH	H	Cl	NO ₂	H	CH ₂ OH	H	H	H	H	>10	ND	ND
41											>10	ND	ND
42											>10	ND	ND

Table 1b
Anti-tumor activity of compounds against MM-1 cell lines



Compd	R ₁	R ₂	R ₃	R ₄	IC ₅₀ (μM)
43		H	H	H	>10
44	Et	H	H	H	>10
45	H	Cl	H	H	>10
46	H	H	H	Me	>10
47	H	H	OMe	H	>10
48					>10

compounds. The first lead was AG1801 from the Levitzki laboratory, which showed higher potency than **AG490** (Table 1a and b). Based on this lead the WP compounds were generated.

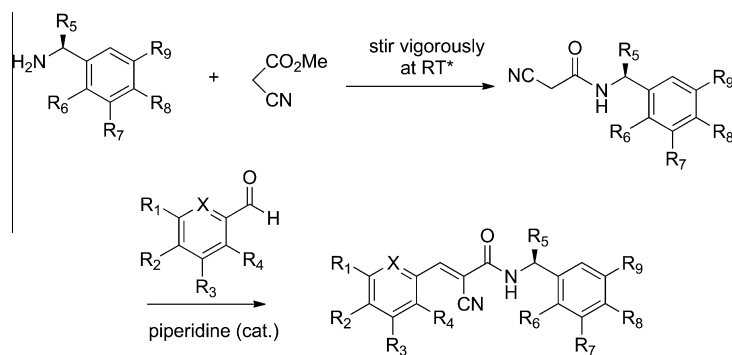
WP1066, is a novel inhibitor structurally related to **AG490** but significantly more potent and active in suppressing Jak2/Stat3 signaling and inducing apoptosis in human malignant glioma U87-MG and U373-MG cells in vitro and in vivo. IC₅₀ values for **WP1066** were 5.6 μM in U87-MG cells and 3.7 μM in U373-MG cells, which represents 18-fold and 8-fold increases in potency, respectively, over that of **AG490** in cellular studies. **WP1066**-mediated apoptosis was associated with activation of Bax, and suppression of c-myc, Bcl-XL and Mcl-1 expression. Systemic intraperitoneal administration of **WP1066** in mice significantly inhibited the growth of subcutaneous malignant glioma.¹³

WP1130 is a close analog of **WP1066** that shows marginal increased potency at the micromolar level against chronic myelogenous leukemia (CML) cells. Compound **WP1130** specifically and rapidly down-regulates both wild-type and T315I mutant Bcr/Abl mutant protein and suppresses the growth of K562 heterotransplanted tumors as well as both wild-type Bcr/Abl and T315I mutant Bcr/Abl-expressing BaF/3 cells transplanted into nude mice.¹⁴ Another published tyrrhostin-like compound, CR4, that

contained an extra-annular double bond added to the existing conjugated system showed submicromolar inhibition against acute lymphocytic leukemia (ALL) cancer cell growth.¹⁵ Our initial work with the MM-1 cell line showed low μM apoptotic and signal transduction inhibitory activity for **WP1066** and **WP1130**. Our aim was to develop analogs of the WP compounds in order to explore the SAR of the tyrrhostin core and its mechanism of action in MM-1 cells. This was accomplished through solution phase synthesis, which was later adapted to solid phase synthesis to expand the molecular diversity of the library and increase the throughput. In our patent application, WO2008005954, we provided a description of the compounds and results in the MM-1 cell line, but did not discuss SAR for each series nor elaborate on the reason for the differences in activity. In this paper, we sought an explanation for the difference in observed activity based on a hypothesis that it was related to nucleophilic attack of the C_β carbon atom. Our recent analysis shows that the more active tyrrhostin derivatives function as deubiquitinase (DUB) inhibitors through a Michael acceptor reaction with the cysteine residue within the DUB active site.^{16,17}

2. Chemistry of tyrrhostin analogs

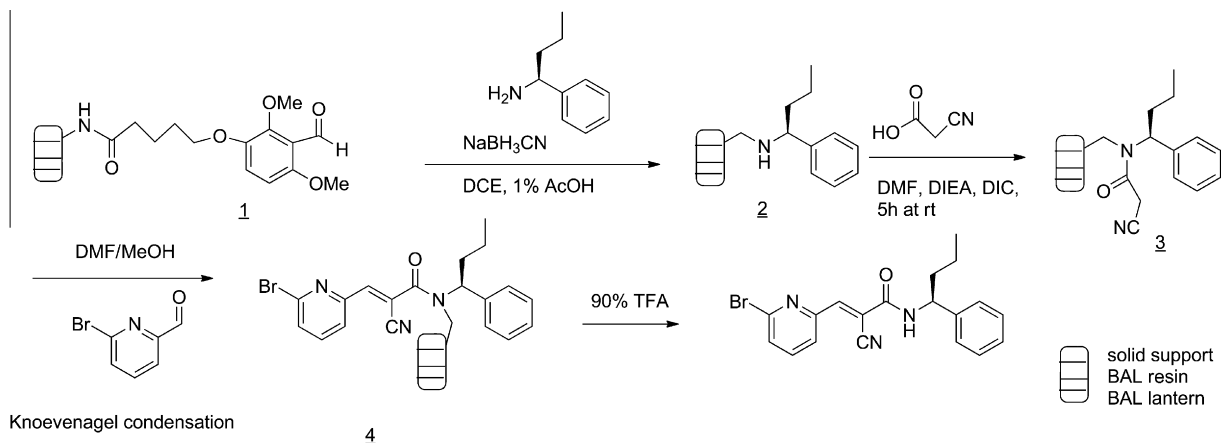
The solution phase synthesis of tyrrhostin analogs were prepared using the procedure shown in Scheme 1. The procedures used were based on tyrrhostin compounds developed by Levitzki et al.¹⁸ First equal molar of benzylamine was coupled with cyanoacetic methyl ester quantitatively to form the *N*-benzylcyanoacetamide as an intermediate, then Knoevenagel condensation with the aldehyde furnished the final product. We synthesized 48 tyrrhostin like compound via solution phase. We expanded on those compounds by adapting the solution phase synthesis to solid support as shown in Scheme 2. The modified procedures were based on those of similar compounds described in the literature.^{19,20} First primary amines were attached to BAL-PG-PS resin (**1**) via a reductive amination reaction. This reaction works much more consistently than direct coupling of amine to bromo-Merrifield resin. The attachment was confirmed by positive control of purple color from ninhydrin test due to the presence of the secondary amine of the attached BAL resin (**2**). Cyano acetic acid was attached to secondary amine BAL resin (**2**) via a DICPDI/DIEA coupling step. A negative ninhydrin color test confirmed the completion of the reaction. TFA cleavage at this step afforded a *N*-benzylcyanoacetamide intermediate, supported by Mass Spectrometry (MS) and NMR analysis. Knoevenagel condensation with benzaldehyde and cyanoacetamide resin (**3**) afforded tyrrhostin compounds attached to the BAL resin (**4**). The



R₁, R₂, R₃, R₄, R₅ and R₆ represent different groups and X=CH, N, or C-NO₂

* sonicate, if necessary

Scheme 1. General procedure for the synthesis of tyrrhostin analogs.



Scheme 2. Solid phase synthesis of tyrphostin analogs.

final compounds were cleaved from BAL resin using 95% TFA. Compound **WP1130** was first successfully synthesized manually on BAL resin and BAL mimotope Lantern (initial specified loading: 750 μmol). Both resin and lantern gave similar yield and purity. Finally, a chemical library of variants of the tyrphostin compound incorporating variability at two sites within the molecule, fifteen at the aldehyde site and six at the amine site (Fig. 2) to make a total of 90 compounds. TLC was used to confirm the presence of major products and MS was tested randomly to confirm the molecular weight of the final tyrphostin compounds. HPLC analyses revealed that the purity of the compounds ranged from 50% to 95% (Supplementary Fig. 1). The synthesized library was screened against the MM-1 cell line without further purification.

3. Biological activity

The synthesized compounds were tested for their ability to inhibit Jak2/Stat3 signal transduction as previously described. Compounds were also assessed for their ability to inhibit cell growth and induce apoptosis as previously described. In those experiments, multiple myeloma (MM-1) was chosen as model for primary screening. Two additional myeloma cell lines (U266, OCI-My4) were used to confirm activity. In a typical experiment, cell lines were incubated with a range of compound concentrations for 72 h to determine the concentration required to inhibit cell growth or induce apoptosis by 50% (IC_{50}) as determined by MTT assays previously described.^{16,17} The IC_{50} values for the compounds against MM-1 cells are listed in

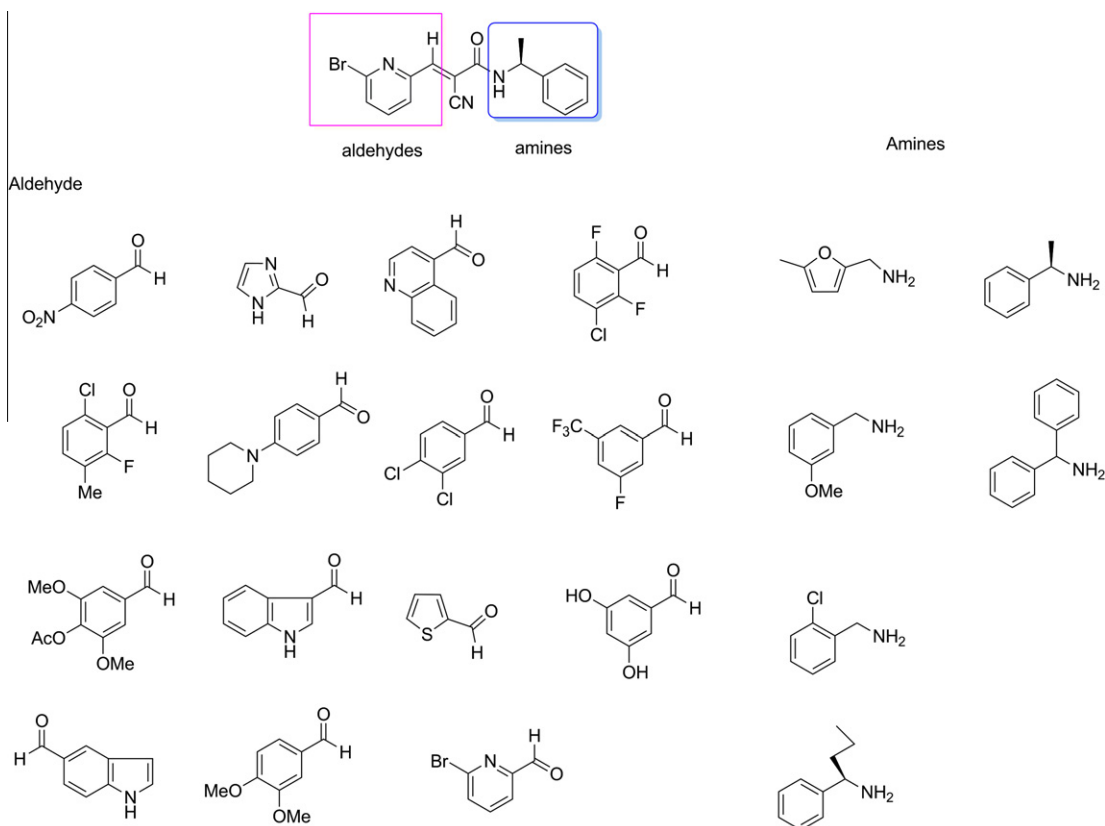


Figure 2. Building blocks used for solid phase library synthesis of tyrphostin analogs.

Table 1a and b. Similar IC₅₀ values were obtained for U266 and OCI-My4 cell lines treated with these compounds.

4. Results and discussion

4.1. Study of SAR

For discussion purposes, series 1 refers to compounds with X = CH; series 2 refers to compounds with X = N and R₁ = Br, and series 3 refers to all others. Even though **WP1066** and **WP1130** had better activity when compared to either **AG490** or **AG1801**, we chose not to bias our search towards either a phenyl or brominated pyridine for the left side. *Series 1*: The activity of the parent **AG490** and **AG1801** were modified by changing both the position and type of substituent on the phenyl ring. In two cases, the activity was nearly the same as that for series 2. Cyclization of the phenyl ring to make a 1,4-benzoxazine or 1,3-benzodioxole (**41**, **42**) seemed to destroy the activity. Replacing the left side with a nitrophenylfuran group (**43–48**) also removed any evidence of activity. *Series 2*: We

Table 2
Theoretical LUMO energies and Fukui f_{NN} values for C_β carbon calculated at the B3LYP/LACV3P** level

Compound	LUMO	Activity	Series	Fukui LUMO f_{NN}
AG1801	-0.128	1	1	0.135
AG490	-0.087	2	1	0.290
WP1066	-0.110	1	2	0.236
WP1130	-0.107	1	2	0.210
5	-0.111	1	2	0.216
6	-0.106	1	2	0.209
7	-0.108	1	2	0.213
8	-0.107	1	2	0.211
9	-0.114	1	2	0.241
10	-0.107	1	2	0.212
11	-0.107	1	2	0.210
12	-0.106	1	2	0.209
13	-0.111	1	2	0.216
15	-0.108	1	2	0.222
16	-0.112	1	2	0.238
17	-0.115	1	2	0.223
18	-0.109	1	2	0.212
19	-0.106	1	2	0.210
20	-0.107	1	2	0.211
21	-0.118	1	1	0.168
22	-0.098	2	1	0.081
23	-0.107	1	2	0.211
24	-0.088	2	1	0.274
25	-0.104	2	2	0.207
26	-0.108	2	2	0.211
27	-0.126	1	1	0.130
28	-0.137	2	1	0.069
29	-0.112	1	1	0.075
30	-0.115	1	1	0.146
31	-0.118	1	1	0.167
32	-0.112	2	1	0.013
33	-0.085	2	1	0.284
34	-0.119	1	1	0.000
35	-0.093	2	1	0.274
36	-0.110	1	2	0.214
37	-0.139	2	1	0.113
38	-0.109	1	2	0.214
39	-0.108	1	2	0.212
40	-0.118	2	1	0.170
41	-0.075	2	3	0.277
42	-0.100	2	3	0.261
43	-0.109	2	3	0.147
44	-0.108	2	3	0.145
45	-0.113	2	3	0.169
46	-0.109	2	3	0.152
47	-0.111	2	3	0.158
48	-0.109	2	3	0.151

Complete set of associated energies, HOMO, and electrophilicity may be found in Supplementary data.

explored modifications to the stereocenter of **WP1130**, to see if replacing the propyl group (Pr) with either smaller or larger groups would lead to better activity. There appeared to be no general trend regarding size since all modifications had decreased or equivalent activity when compared to **WP1130**. However, substitution with a phenyl group (**38**) resulted in a 5 μM inhibitor whereas Bn substitution (**39**) retained activity at 2.5 μM. It is interesting to note that replacing the methyl in **WP1066** with an isosteric CF₃ led to a much larger decrease in activity. Adding a group capable of hydrogen-bond accepting (-CH₂COOCH₃, -CH₂OCOCH₃) as well as donating and accepting (-CH₂OH) led to a small decrease in activity. Cyclizing the RHS (**7**, **8**) to tie up the stereocenter led to a slight decrease in activity; however, this may be balanced by its ability to provide an alternative structural framework for adding other functionality. We found that changing from the configuration (*S*) for the cyclopropyl group at the R₅ position (**23**) to the racemic structure (**20**) did not affect activity. Hydrophobic substitutions at phenyl group from R₆ to R₉ are tolerated; however, an amino substitution removes activity completely. The furan, indole, quinoline structure abolished activity completely. In summary, the left side of tyrphostin compounds is more sensitive than the right side. This makes sense if our hypothesis is true that compound activity is related to the nucleophilic attack at the C_β carbon, since the left side is directly conjugated. In expanding the scope of the tyrphostin analogs, a chemical library of 90 compounds was synthesized from solid phase. No significant increase of activity was observed from the solid phase libraries and it indicates that a plateau has been reached for the current tyrphostin template. In addition, it appears that the phenyl or pyridine heterocycles at the left side (Table 1a and b) are crucial to retain bioactivities in cell line assays.

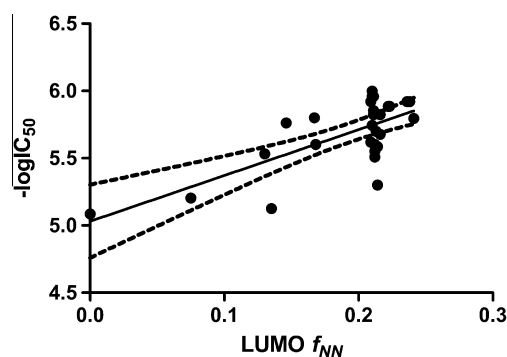


Figure 3. Plot of activity versus Fukui LUMO f_{NN} . 95% confidence levels are shown as dashed lines.

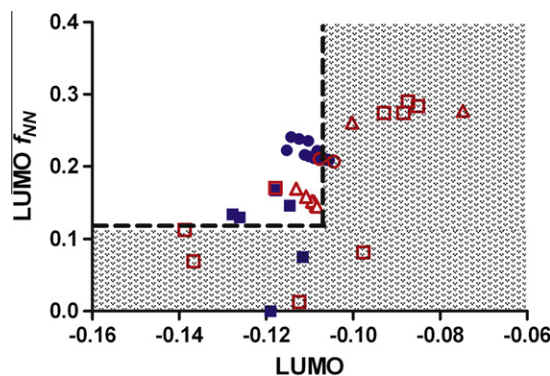


Figure 4. Plot of LUMO f_{NN} versus LUMO energies. Active compounds are solid blue and inactive compounds are outlined in red. Each series is represented by a different shape: rectangle for series 1 with X = C; circle for series 2 with X = N, R₂ = Br; triangle for series 3. Lines were placed at $x = -0.106$ and $y = 0.120$. The patterned area suggests location of inactive compounds.

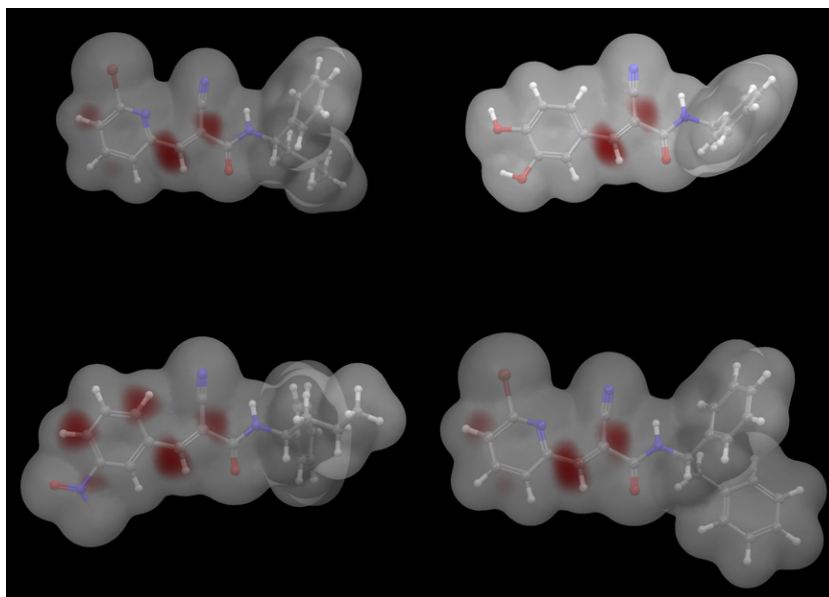


Figure 5. LUMO orbitals mapped onto the electron density surface for (top-left) **WP1130** (top-right) **AG490** (bottom-left) compound **30** (bottom-right) compound **39**. A custom coloring ramp was used that contained red for extremes of negative and positive and white for all other areas.

4.2. Theoretical analysis of reactivity towards nucleophile

The LUMO energies and Fukui function, f_{NN} , calculated at the C_{β} carbon for each compound is listed in Table 2. Structures with IC_{50} values $\leq 10 \mu\text{M}$ in the MM-1 cell line had a moderate correlation ($r^2 = 0.50$, $F = 26.17$, $p = 0.0001$) observed between the experimental $-\log IC_{50}$ values listed in Table 1a and b and the Fukui function, f_{NN} , calculated at the C_{β} carbon as shown in Figure 3. The same analysis done with the U266 and OCI-My4 cell lines showed a correlation of $r^2 = 0.51$ and $r^2 = 0.40$, respectively. Plotting the $-\log IC_{50}$ values for MM-1 cell line versus local electrophilicity, ω_k , also showed a moderate correlation ($r^2 = 0.44$, $F = 20.57$, $p = 0.0001$). This was primarily due to the Fukui function, f_{NN} , since the global electrophilicity index does not correlate well with the $-\log IC_{50}$. A combination of LUMO energies and LUMO f_{NN} values may be used to separate active and inactive compounds. A plot containing this data is shown in Figure 4, with active compounds colored blue and inactive compounds colored red. Generally, if the LUMO is greater than -0.106 or f_{NN} is lower than 0.120 , then the structures were found to be inactive. There are a few exceptions, most of which are in series 3, which we would attribute to steric effects not considered in the Fukui and orbital energy calculations. There are two active compounds shown in the inactive region; however, they have values closer to $10 \mu\text{M}$.

The area's most susceptible to nucleophilic attack may also be described graphically, by mapping the LUMO onto the electron density. This was completed for several molecules as shown in Figure 5. The custom color ramp utilized red-white-red to keep the positive and negative lobes of the orbital the same color and emphasize the most reactive areas. As expected, there is an excellent match of the reactive areas with the LUMO f_{NN} values, especially at the C_{β} and C_{α} carbons. In all compounds, the LUMO f_{NN} for C_{β} is always higher than the value on C_{α} . For **WP1130**, the LUMO f_{NN} for C_{β} and C_{α} carbons are 0.210 and 0.181 , respectively. This may be compared with **AG490**, which has a higher $C_{\beta} = 0.290$ ($C_{\alpha} = 0.153$), and this same difference may be seen in the combination plot. However, **AG490** is not active, which is most likely due to the higher LUMO energy level being mismatched to the nucleophile. Two other actives from Series 1 and Series 2 are also shown in Figure 5. Compound **30** is a molecule in the same series as **AG490** having activity similar to **WP1130**. The overall magnitude

of the LUMO f_{NN} for C_{β} is less (0.146) when compared to **WP1130** due to the additional reactive areas *ortho*- and *para*- to the nitro group. Changing from a propyl in **WP1130** to a much bulkier group in compound **39** has virtually no effect on the reactivity values ($C_{\beta} = 0.212$, $C_{\alpha} = 0.180$) and the graphical representation is nearly identical for both.

5. Conclusion

In conclusion, by expanding upon the SAR of the tyrphostin compounds and analysis of the reactivity of compounds through theoretical calculations, we have found the following:

1. Identified compounds with equivalent activity to WP series, but were not able to identify any with improved activity in the MM-1 cell line.
2. Identified compounds with better activity in Series 1, specifically compounds **21**, **27**, **30**, and **31**.
3. Cyclizing the right-hand side of Series 2 was well tolerated, but did not improve the activity.
4. Changes to the left-hand side of either series resulted in loss of activity.
5. The local electrophilicity and Fukui function, f_{NN} , was moderately correlated with the IC_{50} , suggesting that nucleophilic attack on the C_{β} carbon may involved in explaining the activity differences of such compounds.
6. A general model for separating inactive from active compounds arises from a combination of LUMO energies and Fukui LUMO f_{NN} values.
7. There is an excellent match of the numerical Fukui LUMO f_{NN} values with the graphical representation of reactivity (LUMO mapped onto electron density).

6. Experimental section

6.1. Chemical procedures

All chemicals and solvents were obtained from Sigma–Aldrich (Milwaukee, WI) or Fisher Scientific (Pittsburg, PA) and used without further purification. Analytical HPLC was performed on a

Varian Prostar system, with a Varian Microsorb-MW C18 column (250 × 4.6 mm; 5 μm) using the following solvent system A = H₂O/0.1% TFA and B = acetonitrile/0.1% TFA. Varian Prepstar preparative system equipped with a Prep Microsorb-MW C18 column (250 × 41.4 mm; 6 μm; 60 Å) was used for preparative HPLC with the same solvent systems. Program A: Gradient: 0–5 min. 30% B. 5–35 min. 95% B. 30–35 min. 95% B. Program B: Gradient: 0–5 min. 10% B. 5–35 min. 95% B. 30–40 min. 95% B. Mass spectra (ionspray, a variation of electrospray, unless otherwise noted) were acquired on an Applied Biosystems Q-trap 2000 LC–MS–MS. UV was measured on Perkin Elmer Lambda 25 UV/Vis spectrometer. Solid phase synthesis was performed on apptec apex396 combinatory synthesizer. IR was measured on Perkin Elmer Spectra One FT-IR spectrometer. ¹H NMR and ¹³C NMR spectra were recorded on a Bruker Biospin spectrometer with a B-ACS 60 autosampler: 600.13 MHz for ¹H NMR and 150.92 MHz for ¹³C NMR. Chemical shifts (δ) are determined relative to methanol-d₄ (referenced to 3.34 ppm (δ) for ¹H NMR and 49.86 ppm for ¹³C NMR). Proton–proton coupling constants (J) are given in Hertz and spectral splitting patterns are designated as singlet (s), doublet (d), triplet (t), quadruplet (q), multiplet or overlapped (m), and broad (br). Flash chromatography was performed using Merck Silica Gel 60 (mesh size 230–400 ASTM) or using an Isco (Lincoln, NE) combiFlash Companion or SQ16x flash chromatography system with RediSep columns (normal phase silica gel (mesh size 230–400ASTM)) and Fisher Optima TM grade solvents. Thin-layer chromatography (TLC) was performed on Merck (Darmstadt, Germany) silica gel F-254 aluminum-backed plates with visualization under UV (254 nm) and by staining with potassium permanganate or ceric ammonium molybdate.

6.2. General method for the preparation of tyrphostin analogs (Scheme 1)

In step 1, a mixture of methyl cyanoacetate (25 mmol) and the amine (25 mmol) was stirred vigorously for overnight. The resulting solid was triturated with 8 mL 95% ethanol and the product filtered. The amide from the step1 reaction (5.0 mmol), aldehyde (5 mmol), and piperidine (five drops) were stirred in anhydrous ethanol (10 mL). Ethanol was evaporated and solid was triturated with water and dried under high vacuum to give the desired product.

6.2.1. *N*-(Cyanoacetyl)-1-(4'-aminophenyl)ethyl amide

A mixture of methyl cyanoacetate (2.47 g, 25 mmol) and 1-(4'-aminophenyl)ethylamine (3.40 g 25 mmol) was stirred vigorously for overnight. The resulting solid was triturated with 8 mL 95% ethanol and the product filtered as a white solid (4.08 g, 80% yield). ¹H NMR (600 MHz, CD₃OD) δ 7.12 (dt, 2H, *J* = 2.9, 8.3 Hz), 6.71 (dt, 2H, *J* = 2.9, 8.3 Hz), 4.94 (q, 1H, *J* = 6.7 Hz), 3.2 (s, 2H), 1.43 (d, 3H, 6.4 Hz); ¹³C NMR δ 162.4, 146.9, 132.7, 127.0, 127.0, 115.6, 115.6, 49.4, 20.9.

6.2.2. (*S,E*)-*N*-(1-(4-Bromophenyl)ethyl)-3-(6-bromopyridin-2-yl)-2-cyanoacrylamide (5)

¹H NMR (500 MHz, CDCl₃) δ 8.18 (s, 1H), 7.66 (m, 1H), 7.57 (m, 2H), 7.48 (d, 2H, *J* = 8.4 Hz), 7.24 (d, 2H, *J* = 8.4 Hz), 6.78 (d, 1H, *J* = 6.5 Hz), 5.18 (m, 1H), 1.59 (d, 3H, *J* = 11.8 Hz); ¹³C NMR (125 MHz, CDCl₃) δ 158.61, 150.83, 148.47, 139.16, 131.95, 130.76, 127.91, 125.56, 49.78, 21.63; MS (ESI) *m/e* (rel intensity): 433.8 (50), 435.9 (100), 437.8 (50).

6.2.3. (*S,E*)-3-(6-Bromopyridin-2-yl)-2-cyano-*N*-(1-(4-methoxyphenyl)ethyl)acrylamide (6)

¹H NMR (300 MHz, CDCl₃) δ 8.22 (s, 1H), 7.63 (m, 3H), 7.29 (m, 2H), 6.91 (d, 2H, *J* = 8.6 Hz), 6.73 (d, 1H, *J* = 6.8 Hz), 5.22 (m, 1H),

3.82 (s, 1H), 1.60 (d, 3H, *J* = 6.8 Hz); ¹³C NMR (75 MHz, CDCl₃) δ 159.56, 158.79, 151.33, 148.64, 139.52, 134.50, 131.02, 127.80, 125.78, 114.63, 109.95, 55.72, 50.09, 21.94; MS (ESI) *m/e* (rel intensity): 386.3 (16), 388.3 (16).

6.2.4. (*R,E*)-3-(6-Bromopyridin-2-yl)-2-cyano-*N*-(2,3-dihydro-1*H*-inden-1-yl)acrylamide (7)

¹H NMR (500 MHz, CDCl₃) δ 8.28 (s, 1H), 7.58–7.69 (m, 3H), 7.28 (m, 4H), 6.74 (d, 1H, *J* = 7.8 Hz), 5.62 (m, 1H), 3.07 (m, 1H), 2.94 (m, 1H), 2.70 (m, 1H), 1.95 (m, 1H); ¹³C NMR (125 MHz, CDCl₃) δ 159.22, 150.96, 148.42, 143.44, 142.51, 141.88, 139.16, 130.68, 128.48, 127.08, 125.42, 125.03, 124.06, 115.67, 109.50, 55.97, 33.82, 30.31; MS (ESI) *m/e* (rel intensity): 368.2 (30), 370.2 (30).

6.2.5. (*R,E*)-3-(6-Bromopyridin-2-yl)-2-cyano-*N*-(1,2,3,4-tetrahydronaphthalen-1-yl)acrylamide (8)

¹H NMR (500 MHz, CDCl₃) δ 8.29 (s, 1H), 7.59–7.69 (m, 2H), 7.58 (d, 1H, *J* = 8.5 Hz), 7.19 (m, 2H), 7.13 (d, 1H, *J* = 7.4 Hz), 6.74 (d, 1H, *J* = 8.1 Hz), 5.31 (m, 1H), 2.88 (m, 1H), 2.79 (m, 1H), 2.15 (m, 1H), 1.90 (m, 3H); ¹³C NMR (125 MHz, CDCl₃) δ 158.76, 151.00, 148.40, 142.49, 139.15, 137.65, 135.31, 130.64, 129.43, 128.47, 127.78, 126.54, 125.35, 115.64, 109.69, 48.99, 29.99, 29.13, 20.02; MS (ESI) *m/e* (rel intensity): 382 (50), 384 (50).

6.2.6. (*S,E*)-3-(6-Bromopyridin-2-yl)-*N*-(1-(4-chlorophenyl)ethyl)-2-cyanoacrylamide (9)

¹H NMR (500 MHz, CDCl₃) δ 8.20 (s, 1H), 7.65 (t, 1H, *J* = 7.5 Hz), 7.58 (m, 2H), 7.25 (m, 2H), 7.17 (d, 2H, *J* = 8.0 Hz), 6.75 (d, 1H, *J* = 7.3 Hz), 5.20 (m, 1H), 2.34 (s, 3H), 1.60 (d, 3H, *J* = 6.9 Hz); ¹³C NMR (125 MHz, CDCl₃) δ 158.44, 150.95, 148.36, 142.47, 139.13, 139.07, 137.53, 130.62, 129.55, 126.07, 125.40, 115.73, 109.56, 50.03, 21.67, 21.07; MS (ESI) *m/e* (rel intensity): 370.2 (47), 372.2 (50).

6.2.7. (*R,E*)-3-(6-Bromopyridin-2-yl)-2-cyano-*N*-(2-hydroxy-1-phenylethyl)acrylamide (10)

¹H NMR (500 MHz, DMSO-*d*₆) δ 8.82 (d, 1H, *J* = 7.9 Hz), 8.10 (s, 1H), 7.95 (t, 1H, *J* = 7.7 Hz), 7.89 (d, 1H, *J* = 7.3 Hz), 7.80 (d, 1H, *J* = 7.8 Hz), 7.38 (d, 2H, *J* = 7.2 Hz), 7.34 (m, 2H), 7.26 (t, 1H, *J* = 7.2 Hz), 5.02 (t, 1H, *J* = 5.7 Hz), 4.97 (m, 1H), 3.68 (m, 2H); ¹³C NMR (125 MHz, DMSO-*d*₆) δ 161.26, 151.59, 146.67, 141.67, 141.20, 140.77, 130.97, 128.70, 127.56, 127.43, 126.66, 115.53, 111.34, 64.63, 56.94; MS (ESI) *m/e* (rel intensity): 372.3 (89), 374.2 (100).

6.2.8. (*S,E*)-3-(6-Bromopyridin-2-yl)-2-cyano-*N*-(1-phenylpropyl)acrylamide (11)

¹H NMR (500 MHz, CDCl₃) δ 8.19 (s, 1H), 7.65 (dd, 1H, *J* = 5.0, 4.3 Hz), 7.57 (d, 2H, *J* = 4.7 Hz), 7.27–7.38 (m, 3H), 6.78 (d, 1H, *J* = 4.8 Hz), 4.99 (m, 1H), 1.94 (m, 1H), 0.95 (d, 3H, *J* = 5.4 Hz); ¹³C NMR (125 MHz, CDCl₃) δ 158.67, 150.92, 148.26, 142.48, 141.01, 139.12, 130.64, 128.84, 127.76, 126.58, 125.41, 115.81, 109.54, 56.34, 29.09, 10.69; MS (ESI) *m/e* (rel intensity): 370.1 (90), 372.1 (100).

6.2.9. (*S,E*)-3-(6-Bromopyridin-2-yl)-2-cyano-*N*-(1-(3-methoxyphenyl)ethyl)acrylamide (12)

¹H NMR (500 MHz, CDCl₃) δ 8.23 (s, 1H), 7.68 (t, 1H, *J* = 7.8 Hz), 7.60 (m, 2H), 7.31 (t, 1H, *J* = 7.9 Hz), 6.96 (d, 1H, *J* = 8.0 Hz), 6.91 (m, 1H), 6.85 (dd, 1H, *J* = 8.2, 2.5 Hz), 6.79 (d, 1H, *J* = 7.6 Hz), 5.23 (m, 1H), 3.84 (s, 3H), 1.62 (d, 3H, *J* = 6.9 Hz); ¹³C NMR (125 MHz, CDCl₃) δ 159.99, 158.51, 150.91, 148.34, 143.68, 142.47, 139.14, 130.66, 129.97, 125.43, 118.30, 115.74, 113.03, 112.12, 109.47, 55.27, 50.23, 21.707; MS (ESI) *m/e* (rel intensity): 386.2 (50), 388.2 (53).

6.2.10. (S,E)-3-(6-Bromopyridin-2-yl)-N-(1-(4-chlorophenyl)ethyl)-2-cyanoacrylamide (13)

¹H NMR (500 MHz, CDCl₃) δ 8.19 (s, 1H), 7.65 (m, 1H), 7.58 (m, 2H), 7.33 (d, 2H, *J* = 8.6 Hz), 7.27 (d, 2H, *J* = 8.6 Hz), 6.75 (d, 1H, *J* = 6.5 Hz), 5.20 (m, 1H), 1.59 (d, 3H, *J* = 6.9 Hz); ¹³C NMR (125 MHz, CDCl₃) δ 158.61, 150.80, 148.46, 142.50, 140.67, 139.15, 133.56, 130.76, 129.00, 127.56, 125.53, 115.72, 109.24, 49.70, 21.66; MS (ESI) *m/e* (rel intensity): 390 (70), 392 (85).

6.2.11. (R,E)-3-(6-Bromopyridin-2-yl)-2-cyano-N-(2,2,2-trifluoro-1-phenylethyl)acrylamide (14)

¹H NMR (300 MHz, CDCl₃) δ 8.25 (s, 1H) 7.69 (m, 1H), 7.45 (s, 5H), 7.61 (m, 2H), 7.16 (d, 1H, *J* = 9.5 Hz), 5.80 (m, 1H); MS (ESI) *m/e* (rel intensity): 410.2 (94), 412.2 (100), 429.1 (28).

6.2.12. (S,E)-3-(6-Bromopyridin-2-yl)-2-cyano-N-(1-(3-(trifluoromethyl)phenyl)ethyl)acrylamide (15)

¹H NMR (500 MHz, CDCl₃) δ 8.22 (s, 1H), 7.69 (m, 1H), 7.60 (m, 2H), 7.51 (m, 1H), 6.88 (d, 1H, *J* = 8.4 Hz), 5.31 (m, 1H), 1.66 (d, 3H, *J* = 8.4 Hz); ¹³C NMR (125 MHz, CDCl₃) δ 158.74, 150.75, 148.60, 143.26, 142.50, 139.16, 130.80, 129.53, 129.37, 125.61, 124.62, 123.02, 122.99, 122.89, 115.70, 109.10, 49.94, 21.68; MS (EI) *m/e* (rel intensity): 422.0 (53), 424.0 (67).

6.2.13. (S,E)-3-(6-Bromopyridin-2-yl)-2-cyano-N-(1-(4-fluorophenyl)ethyl)acrylamide (16)

¹H NMR (500 MHz, CDCl₃) δ 8.20 (s, 1H), 7.69 (m, 1H), 7.60 (m, 2H), 7.36 (m, 2H), 7.08 (m, 2H), 6.78 (d, 1H, *J* = 8.4 Hz), 5.24 (t, 1H, *J* = 8.4 Hz), 1.62 (d, 3H, *J* = 8.4 Hz); ¹³C NMR (125 MHz, CDCl₃) δ 163.28, 161.32, 158.62, 150.91, 148.49, 142.57, 139.22, 137.98, 130.80, 127.98, 127.91, 125.57, 115.87, 115.80, 115.70, 109.41, 49.70, 21.77; MS (EI) *m/e* (rel intensity): 374.3 (11), 376.3 (11).

6.2.14. (S,E)-N-(1-(3,5-bis(trifluoromethyl)phenyl)ethyl)-3-(6-bromopyridin-2-yl)-2-cyanoacrylamide (17)

¹H NMR (500 MHz, CDCl₃) δ 8.18 (s, 1H), 7.80 (s, 1H), 7.60 (m, 2H), 7.67 (m, 2H), 7.57 (m, 1H), 6.92 (d, 1H, *J* = 8.4 Hz), 5.31 (m, 1H), 1.67 (d, 3H, *J* = 8.4 Hz); ¹³C NMR (125 MHz, CDCl₃) δ 158.74, 150.75, 148.60, 143.26, 142.50, 139.16, 130.80, 129.53, 129.37, 125.61, 124.62, 123.02, 122.99, 122.89, 115.70, 109.10, 49.94, 21.68; MS (EI) *m/e* (rel intensity): 490.1 (86), 492.1 (100).

6.2.15. (S,E)-Methyl 3-(3-(6-bromopyridin-2-yl)-2-cyanoacrylamido)-3-phenylpropanoate (18)

¹H NMR (300 MHz, CDCl₃) δ 8.20 (s, 1H), 7.76 (d, 1H, *J* = 7.8 Hz), 7.62 (m, 3H), 7.32 (m, 5H), 5.52 (m, 1H), 3.70 (s, 1H), 2.98 (m, 2H); ¹³C NMR (125 MHz, CDCl₃) δ 171.03, 158.84, 150.90, 148.51, 142.49, 139.56, 139.17, 130.70, 128.96, 128.09, 126.24, 125.39, 115.55, 109.48, 52.11, 50.82, 39.73.

6.2.16. (S,E)-3-(6-Bromopyridin-2-yl)-2-cyano-N-(1-(2-fluorophenyl)ethyl)acrylamide (19)

¹H NMR (500 MHz, CDCl₃) δ 8.19 (s, 1H), 7.66 (m, 1H), 7.58 (m, 2H), 7.31 (m, 2H), 7.14 (t, 1H, *J* = 7.5 Hz), 7.08 (m, 1H), 6.99 (d, 1H, *J* = 7.0 Hz), 5.41 (m, 1H, *J* = 8.4 Hz), 1.61 (d, 3H, *J* = 7.0 Hz); ¹³C NMR (150 MHz, CDCl₃) δ 161.45, 159.82, 158.47, 150.88, 148.40, 142.45, 139.18, 130.68, 129.43, 129.37, 129.16, 129.07, 127.87, 127.84, 125.47, 124.51, 124.49, 116.16, 116.02, 115.65, 109.38, 46.53, 21.29.

6.2.17. (E)-3-(6-Bromopyridin-2-yl)-2-cyano-N-(cyclopropyl(phenyl)methyl)acrylamide (20)

¹H NMR (600 MHz, CDCl₃) δ 8.20 (s, 1H), 7.67 (t, 1H, *J* = 7.8 Hz), 7.58 (m, 2H), 7.38 (m, 4H), 7.30 (m, 1H), 6.99 (d, 1H, *J* = 7.8 Hz), 4.51 (t, 1H, *J* = 8.4 Hz), 1.29 (m, 1H), 0.68 (m, 2H), 0.50 (m, 1H), 0.44 (m, 1H); ¹³C NMR (600 MHz, CDCl₃) δ 158.22, 148.96,

140.66, 133.57, 133.05, 131.62, 130.97, 128.85, 127.94, 127.24, 126.71, 115.99, 107.83, 59.15, 16.69, 4.26, 4.20; MS (EI) *m/e* (rel intensity): 382.2 (60).

6.2.18. (E)-3-(4-Chloro-3-nitrophenyl)-2-cyano-N-(cyclopropyl(phenyl)methyl)acrylamide (21)

¹H NMR (600 MHz, CDCl₃) δ 8.33 (d, 1H, *J* = 1.8 Hz), 8.28 (s, 1H), 8.08 (dd, 1H, *J* = 8.4, 2.4 Hz), 7.69 (d, 1H, *J* = 8.4 Hz), 7.36–7.40 (m, 4H), 7.31 (m, 1H), 6.80 (d, 1H, *J* = 7.8 Hz), 4.50 (t, 1H, *J* = 8.4 Hz), 1.30 (m, 1H), 0.68 (m, 2H), 0.51 (m, 1H), 0.44 (m, 1H); ¹³C NMR (600 MHz, CDCl₃) δ 158.22, 148.96, 140.66, 133.57, 133.05, 131.62, 130.97, 128.85, 127.94, 127.24, 126.71, 115.99, 107.83, 59.15, 16.69, 4.26, 4.20; MS (EI) *m/e* (rel intensity): 382.2 (60).

6.2.19. (E)-2-Cyano-N-(cyclopropyl(phenyl)methyl)-3-(3-nitro-4-(piperidin-1-yl)phenyl)acrylamide (22)

¹H NMR (600 MHz, CDCl₃) δ 8.24 (s, 1H), 8.15 (s, 1H), 8.08 (d, 1H, *J* = 9.0 Hz), 7.35–7.40 (m, 4H), 7.29 (t, 1H, *J* = 7.2 Hz), 7.10 (d, 1H, *J* = 9.0 Hz), 6.72 (d, 1H, *J* = 7.8 Hz), 4.50 (t, 1H, *J* = 8.4 Hz), 3.22 (m, 4H), 1.72 (m, 4H), 1.68 (m, 2H), 1.58 (s, 2H), 1.27 (m, 1H), 0.66 (m, 2H), 0.51 (m, 1H), 0.43 (m, 1H);

¹³C NMR (600 MHz, CDCl₃) δ 159.81, 150.54, 148.55, 141.16, 139.18, 134.16, 131.05, 128.74, 127.72, 126.73, 121.62, 119.97, 117.94, 101.13, 58.72, 51.87, 25.64, 23.80, 16.77, 4.22, 4.11; MS (ESI) *m/e* (rel intensity): 431.3 (100).

6.2.20. (S,E)-3-(6-Bromopyridin-2-yl)-2-cyano-N-(cyclopropyl(phenyl)methyl)acrylamide (23)

MS (EI) *m/e* (rel intensity): 382.3 (42), 384.3 (31), 399.2 (19), 401.2 (22), 414.3 (45).

6.2.21. (E)-2-Cyano-N-(cyclopropyl(phenyl)methyl)-3-(4-hexylphenyl)acrylamide (24)

¹H NMR (600 MHz, CDCl₃) δ 8.24 (s, 1H), 7.91 (d, 1H, *J* = 9.0 Hz), 7.35–7.41 (m, 4H), 7.29 (m, 1H), 6.96 (d, 1H, *J* = 9.0 Hz), 6.73 (d, 1H, *J* = 7.8 Hz), 4.51 (t, 1H, *J* = 8.4 Hz), 4.03 (m, 2H), 1.80 (m, 2H), 1.46 (m, 2H), 1.35 (m, 4H), 1.26 (m, 1H), 0.91 (t, 1H, *J* = 6.6 Hz), 0.66 (m, 2H), 0.51 (m, 1H), 0.44 (m, 1H).

6.2.22. (S,E)-N-(1-(4-Aminophenyl)ethyl)-3-(6-bromopyridin-2-yl)-2-cyanoacrylamide (25)

The amide from the previous reaction (1.2 g, 5.2 mmol), 6-bromo-pyridinecarboxylaldehyde (0.97 g, 5.2 mmol) and piperidine (five drops) were stirred in anhydrous ethanol (10 mL). Ethanol was evaporated and solid was triturated with water and dried under high vacuum to give (1.7 g, 82% yield) of the desired product as a white solid; ¹H NMR (600 MHz, DMSO-*d*₆) δ 8.72 (d, 1H, *J* = 7.8 Hz), 8.57 (s, 1H), 8.15 (d, 1H, *J* = 7.6 Hz), 7.91 (t, 1H, *J* = 7.8 Hz), 7.79 (d, 1H, 7.8 Hz), 7.36 (m, 4H), 4.93 (p, 1H, *J* = 7.2 Hz), 3.68 (s, 1H), 1.38 (d, 3H, *J* = 7.0 Hz); ¹³C NMR δ 162.1, 159.5, 156.1, 149.5, 143.8, 142.1, 141.2, 130.7, 127.8, 122.3, 121.7, 117.1, 49.2, 26.3, 23.0; MS (C₁₇H₁₅BrN₄O) estimated 370.04 found, 371.2 and 373.2 (M+H).

6.2.23. (E)-N-(3-Aminobenzyl)-3-(6-bromopyridin-2-yl)-2-cyanoacrylamide (26)

¹H NMR (600 MHz, DMSO-*d*₆) δ 8.74 (t, 1H, *J* = 5.6 Hz), 8.57 (s, 1H), 7.15 (d, 1H, *J* = 10.1 Hz), 7.91 (t, 1H, *J* = 7.8 Hz), 7.84 (d, 1H, *J* = 7.8 Hz), 7.35 (s, 4H), 4.32 (d, 2H, *J* = 5.8 Hz), 3.7 (s, 2H); MS (C₁₆H₁₃BrN₄O) estimated 356.03 found, 355.3 and 357.3 (M+H).

6.2.24. (S,E)-2-Cyano-3-(4-nitrophenyl)-N-(1-phenylbutyl)acrylamide (27)

¹H NMR (600 MHz, CDCl₃) δ 9.08 (d, 1H, 2.1 Hz), 8.73 (s, 1H), 8.60 (dd, 1H, *J* = 6.0, 2.1 Hz), 7.32 (m, 5H), 6.6 (d, 2H, *J* = 8.1 Hz), 5.08 (q, 1H, *J* = 7.5 Hz), 1.90 (m, 2H), 1.46 (m, 2H), 0.96 (t, 3H, *J* = 7.5 Hz); ¹³C

NMR δ 157.1, 151.2, 148.7, 140.9, 134.4, 132.2, 128.9, 128.9, 128.5, 127.9, 126.6, 126.6, 120.9, 115.4, 110.0, 54.9, 38.0, 19.5, 13.7; MS ($C_{20}H_{19}N_3O_3$) estimated 349.14 found, 350.2 (M+H).

6.2.25. (S,E)-2-Cyano-3-(2,4-dinitrophenyl)-N-(1-phenylbutyl)acrylamide (28)

1H NMR (600 MHz, $CDCl_3$) δ 9.11 (d, 1H, $J = 1.0$ Hz), 8.76 (s, 1H), 8.64 (dd, 1H, $J = 4.5, 1.2$ Hz), 7.98 (d, 1H, $J = 4.2$ Hz), 7.35 (m, 5H), 6.58 (d, 1H, $J = 3.9$ Hz), 5.10 (q, 1H, $J = 7.5$ Hz), 1.93 (m, 2H), 1.39 (m, 2H), 0.99 (t, 3H, $J = 7.5$ Hz); ^{13}C NMR δ 157.1, 149.1, 148.7, 140.9, 134.4, 132.0, 128.9, 128.9, 128.5, 128.0, 127.9, 126.6, 126.6, 120.9, 114.6, 112.3, 54.9, 38.0, 19.5, 13.7; MS ($C_{20}H_{18}N_4O_5$) estimated 394.12 found, 393.2 (M–H).

6.2.26. (S,E)-2-Cyano-3-(2-nitrophenyl)-N-(1-phenylbutyl)acrylamide (29)

1H NMR (600 MHz, $CDCl_3$) δ 8.71 (d, 1H, $J = 2.0$ Hz), 8.23 (dd, 1H, $J = 4.5, 1.2$ Hz), 7.75 (d, 2H, $J = 4.2$ Hz), 7.65 (m, 1H), 7.35 (m, 4H), 7.29 (m, 1H), 6.68 (m, 1H), 5.09 (q, 1H, $J = 7.5$ Hz), 1.89 (m, 2H), 1.37 (m, 2H), 0.93 (t, 3H, $J = 7.5$ Hz); ^{13}C NMR δ 158.1, 151.2, 147.5, 141.3, 134.4, 131.8, 130.4, 128.8, 128.8, 128.7, 127.7, 126.7, 126.7, 125.4, 115.4, 110.0, 54.7, 38.1, 19.5, 13.8; MS ($C_{20}H_{19}N_3O_3$) estimated 349.14 found, 348.5 (M–H).

6.2.27. (S,E)-2-Cyano-3-(3-nitrophenyl)-N-(1-phenylbutyl)acrylamide (30)

1H NMR (600 MHz, $CDCl_3$) δ 8.68 (d, 1H, $J = 1.8$ Hz), 8.36 (m, 2H), 8.24 (d, 1H, $J = 7.8$ Hz), 7.70 (t, 1H, $J = 7.8$ Hz), 7.33 (m, 5H), 6.62 (d, 1H, $J = 7.8$ Hz), 5.08 (q, 1H, $J = 7.2$ Hz), 1.90 (m, 2H), 1.38 (m, 2H), 0.96 (t, 3H, $J = 7.2$ Hz); ^{13}C NMR δ 158.3, 150.1, 148.7, 141.2, 135.1, 133.4, 130.4, 128.9, 128.9, 127.8, 126.6, 126.5, 125.2, 116.0, 107.7, 54.8, 38.1, 19.5, 13.7; MS ($C_{20}H_{19}N_3O_3$) estimated 349.14 found, 348.3 (M–H).

6.2.28. (S,E)-3-(4-Chloro-3-nitrophenyl)-2-cyano-N-(1-phenylbutyl)acrylamide (31)

1H NMR (600 MHz, $CDCl_3$) δ 8.32 (d, 1H, $J = 2.4$ Hz), 8.26 (s, 1H), 8.07 (dd, 1H, $J = 6.0, 1.8$ Hz), 7.68 (d, 1H, $J = 8.4$ Hz), 7.31 (m, 5H), 6.58 (d, 1H, $J = 7.8$ Hz), 5.08 (q, 1H, $J = 7.2$ Hz), 1.90 (m, 2H), 1.38 (m, 2H), 0.96 (t, 3H, $J = 7.2$ Hz); ^{13}C NMR δ 158.1, 148.7, 147.5, 141.1, 133.5, 132.9, 131.6, 130.8, 128.9, 128.9, 127.8, 127.1, 126.5, 126.5, 115.9, 107.8, 54.8, 38.1, 19.5, 13.7; MS ($C_{20}H_{18}ClN_3O_3$) estimated 383.10 found, 384.2 (M+H).

6.2.29. (S,E)-3-(2-Chloro-6-nitrophenyl)-2-cyano-N-(1-phenylbutyl)acrylamide (32)

1H NMR (600 MHz, $CDCl_3$) δ 8.54 (s, 1H), 8.16 (d, 1H, $J = 8.4$ Hz), 7.82 (d, 1H, $J = 7.8$ Hz), 7.59 (t, 1H, $J = 8.4$ Hz), 7.36 (m, 5H), 6.62 (d, 1H, $J = 7.8$ Hz), 5.10 (q, 1H, $J = 7.2$ Hz), 1.90 (m, 2H), 1.36 (m, 2H), 0.97 (t, 3H, $J = 7.2$ Hz); ^{13}C NMR δ 157.4, 149.0, 148.3, 141.1, 135.5, 134.7, 131.1, 128.9, 128.9, 128.0, 127.8, 126.7, 126.7, 123.8, 114.2, 113.5, 54.8, 38.1, 19.5, 13.8; MS ($C_{20}H_{18}ClN_3O_3$) estimated 383.10 found, 382.2 (M–H).

6.2.30. (S,E)-2-Cyano-3-(4-hydroxyphenyl)-N-(1-phenylbutyl)acrylamide (33)

1H NMR (600 MHz, $CDCl_3$) δ 8.14 (s, 1H), 7.86 (dd, 2H, $J = 6.0, 2.1$ Hz), 7.32 (m, 5H), 6.7 (d, 2H, $J = 8.1$ Hz), 6.62 (d, 1H, $J = 7.8$ Hz), 5.08 (q, 1H, $J = 7.2$ Hz), 1.90 (m, 2H), 1.46 (m, 2H), 0.96 (t, 3H, $J = 7.5$ Hz); ^{13}C NMR δ 160.9, 157.0, 155.7, 151.2, 144.1, 135.2, 132.0, 131.4, 128.9, 127.7, 126.5, 126.5, 125.9, 117.0, 111.1, 54.8, 38.3, 19.5, 13.7; MS ($C_{20}H_{20}N_2O_2$) estimated 320.15 found, 321.6 (M+H).

6.2.31. (S,E)-2-Cyano-3-(4-hydroxy-3-nitrophenyl)-N-(1-phenylbutyl)acrylamide (34)

1H NMR (600 MHz, $CDCl_3$) δ 8.25 (s, 1H), 7.20 (d, 1H, $J = 9.0$ Hz), 7.60 (s, 1H), 7.49 (d, 1H, $J = 8.4$ Hz), 7.33 (m, 5H), 6.65 (d, 1H, $J = 7.8$ Hz), 5.07 (q, 1H, $J = 7.2$ Hz), 1.90 (m, 2H), 1.44 (m, 2H), 0.97 (t, 3H, $J = 7.5$ Hz); ^{13}C NMR δ 158.1, 154.9, 149.8, 141.1, 139.9, 134.8, 132.9, 131.6, 130.8, 128.9, 128.9, 127.8, 126.5, 126.5, 126.0, 121.9, 120.9, 115.8, 109.2, 54.8, 38.1, 19.5, 13.7; MS ($C_{20}H_{19}N_3O_4$) estimated 365.137 found, 366.5 (M+H).

6.2.32. (S,E)-3-(3-Bromo-4-hydroxyphenyl)-2-cyano-N-(1-phenylbutyl)acrylamide (35)

1H NMR (600 MHz, $CDCl_3$) δ 8.13 (s, 1H), 8.03 (s, 1H), 7.20 (d, 1H, $J = 8.4$ Hz), 7.30 (m, 5H), 7.05 (dd, 1H, $J = 8.4, 0.6$ Hz), 6.59 (d, 1H, $J = 7.8$ Hz), 5.07 (q, 1H, $J = 7.2$ Hz), 1.90 (m, 2H), 1.44 (m, 2H), 0.97 (t, 3H, $J = 7.5$ Hz); ^{13}C NMR δ 156.6, 153.6, 141.1, 137.7, 132.9, 130.6, 130.4, 130.4, 128.9, 127.8, 126.5, 126.5, 123.5, 122.3, 122.2, 120.6, 116.9, 114.8, 54.9, 38.2, 19.5, 13.7; MS ($C_{20}H_{19}BrN_2O_2$) estimated 398.06 found, 399.4 and 401.2 (M+H).

6.2.33. (R,E)-2-(3-(6-Bromopyridin-2-yl)-2-cyanoacrylamido)-2-phenylethyl acetate (36)

1H NMR (600 MHz, $CDCl_3$) δ 8.20 (s, 1H), 7.67 (m, 1H), 7.59 (m, 2H), 7.38 (m, 5H), 7.28 (d, 1H, $J = 8.4$ Hz), 6.50 (d, 1H, $J = 7.2$ Hz), 5.39 (m, 1H), 4.44 (m, 2H), 2.08 (s, 3H); ^{13}C NMR δ 171.0, 159.1, 150.7, 148.6, 142.5, 139.2, 137.3, 130.8, 129.0, 129.0, 128.4, 126.7, 126.7, 125.6, 115.6, 109.2, 65.8, 53.7, 20.8; MS ($C_{19}H_{16}BrN_3O_3$) estimated 413.037 found, 414.1 and 416.1 (M+H).

6.2.34. (S,E)-2-Cyano-3-(3,4-dinitrophenyl)-N-(1-phenylethyl)acrylamide (37)

1H NMR (600 MHz, $CDCl_3$) δ 8.23 (s, 1H), 8.16 (s, 1H), 8.08 (d, 1H, $J = 9.0$ Hz), 7.37 (m, 5H), 7.10 (d, 1H, $J = 9.0$ Hz), 5.23 (d, 1H, $J = 7.2$ Hz), 1.59 (d, 3H, $J = 7.2$ Hz); MS ($C_{18}H_{14}N_4O_5$) estimated 366.096 found, 367.2 (M+H).

6.2.35. (E)-N-Benzhydryl-3-(6-bromopyridin-2-yl)-2-cyanoacrylamide (38)

1H NMR (600 MHz, $CDCl_3$) δ 8.26 (s, 1H), 7.67 (m, 1H), 7.59 (m, 2H), 7.38 (m, 5H), 7.33 (m, 11H), 6.50 (d, 1H, $J = 7.2$ Hz); ^{13}C NMR δ 158.8, 150.8, 148.8, 142.5, 140.3, 139.2, 130.8, 129.1, 129.0 (4C), 128.3 (2C), 128.0, 127.4 (4C), 126.9, 125.7, 115.7, 109.1, 58.2; MS ($C_{22}H_{16}BrN_3O$) estimated 417.047 found, 418.1 and 420.1 (M+H).

6.2.36. (E)-3-(6-Bromopyridin-2-yl)-2-cyano-N-(1,2-diphenylethyl)acrylamide (39)

1H NMR (600 MHz, $CDCl_3$) δ 8.06 (s, 1H), 7.56 (t, 1H, $J = 7.8$ Hz), 7.50 (d, 1H, $J = 7.8$ Hz), 7.45 (d, 1H, $J = 7.8$ Hz), 7.20 (m, 10H), 5.34 (q, 1H, $J = 7.2$ Hz), 3.19 (m, 2H); ^{13}C NMR δ 158.8, 150.8, 148.3, 142.4, 140.8, 139.3, 136.8, 130.7, 129.4 (2C), 128.8 (2C), 128.7 (2C), 127.8, 126.9, 126.6 (2C), 125.8, 115.7, 109.1, 56.0, 42.5; MS ($C_{23}H_{18}BrN_3O$) estimated 431.063 found, 432.2 and 434.2 (M+H).

6.2.37. (R,E)-3-(4-Chloro-3-nitrophenyl)-2-cyano-N-(2-hydroxy-1-phenylethyl)acrylamide (40)

1H NMR (600 MHz, $DMSO-d_6$) δ 8.32 (d, 1H, $J = 8.4$ Hz), 8.13 (s, 1H), 8.08 (dd, 1H, $J = 9.0, 2.4$ Hz), 7.36 (m, 4H), 7.30 (m, 1H), 7.08 (d, 1H, $J = 8.4$ Hz), 7.04 (d, 1H, $J = 6.6$ Hz), 5.20 (q, 1H, $J = 7.2$ Hz), 3.96 (m, 2H), 2.08 (s, 3H); ^{13}C NMR δ 160.9, 150.7, 148.6, 139.0, 138.3, 134.1, 131.2, 130.8, 129.0, 129.0, 128.2, 126.7, 126.7, 125.6, 121.4, 119.9, 117.3, 100.8, 65.9, 56.5, 20.8; MS ($C_{18}H_{14}ClN_3O_4$) estimated 371.067 found, 372.2 (M+H).

6.2.38. (S,E)-2-Cyano-3-(4-methyl-3,4-dihydro-2H-benzo[b][1,4]oxazin-7-yl)-N-(1-phenylethyl)acrylamide (41)

¹H NMR (600 MHz, CDCl₃) δ 8.06 (s, 1H), 7.47 (d, 1H, *J* = 1.2 Hz), 7.42 (dd, 1H, *J* = 9.0, 2.4 Hz), 7.33 (m, 4H), 7.27 (m, 1H), 6.60 (d, 1H, *J* = 8.4 Hz), 6.51 (d, 1H, *J* = 6.6 Hz), 5.20 (p, 1H, *J* = 7.2 Hz), 4.22 (t, 2H, *J* = 4.8 Hz), 3.41 (t, 2H, *J* = 4.8 Hz), 2.99 (s, 3H), 1.56 (d, 3H, *J* = 6.6 Hz); ¹³C NMR δ 160.4, 152.7, 143.2, 142.8, 131.7, 128.8 (2C), 128.2, 127.6, 126.2, 126.1 (2C), 120.9, 118.6, 117.2, 110.8, 63.8, 49.9, 48.7, 38.1, 21.5; MS (C₂₁H₂₁N₃O₂) estimated 347.163 found, 348.3 (M+H).

6.2.39. (S,E)-2-Cyano-3-(2,2-difluorobenzo[d][1,3]dioxol-5-yl)-N-(1-phenylethyl)acrylamide (42)

¹H NMR (600 MHz, CDCl₃) δ 8.26 (s, 1H), 7.79 (d, 1H, *J* = 1.2 Hz), 7.82 (d, 1H, *J* = 7.8 Hz), 7.58 (dd, 1H, *J* = 8.4, 1.8 Hz), 7.36 (m, 4H), 7.30 (m, 1H), 7.17 (d, 1H, *J* = 8.4 Hz), 6.56 (d, 1H, *J* = 6.6 Hz), 5.24 (p, 1H, *J* = 7.2 Hz), 1.60 (d, 3H, *J* = 6.6 Hz); ¹³C NMR δ 158.9, 151.5, 146.6, 144.4, 142.1, 131.7, 128.9 (4C), 128.1, 127.9, 126.2 (2C), 116.7, 110.1, 103.9, 50.3, 21.7; MS (C₁₉H₁₄F₂N₂O₃) estimated 356.097 found, 358.1 (M+H).

6.2.40. (E)-2-Cyano-N-(cyclopropyl(phenyl)methyl)-3-(5-(3-nitrophenyl)furan-2-yl)acrylamide (43)

¹H NMR (600 MHz, CDCl₃) δ 8.63 (s, 1H), 8.23 (d, 1H, *J* = 8.4 Hz), 8.19 (d, 1H, *J* = 7.8 Hz), 8.06 (s, 1H), 7.68 (t, 1H, *J* = 7.2 Hz), 7.39 (m, 4H), 7.30 (t, 1H, *J* = 6.6 Hz), 7.20 (s, 1H), 7.05 (d, 1H, *J* = 2.4 Hz), 6.80 (d, 1H, *J* = 7.2 Hz), 4.52 (t, 1H, *J* = 8.4 Hz), 1.28 (m, 1H), 0.68 (m, 2H), 0.52 (m, 1H), 0.44 (m, 1H); ¹³C NMR (600 MHz, CDCl₃) δ 159.53, 149.03, 156.06, 148.78, 141.03, 136.41, 130.50, 130.45, 128.70, 127.69, 126.65, 123.72, 123.32, 120.91, 119.87, 117.19, 112.54, 110.38, 100.54, 58.70, 16.74, 4.19, 4.03; MS (EI) *m/e* (rel intensity): 414.6 (100), 431.4 (42).

6.2.41. (S,E)-2-Cyano-3-(5-(3-nitrophenyl)furan-2-yl)-N-(1-phenylpropyl)acrylamide (44)

¹H NMR (600 MHz, CDCl₃) δ 8.63 (s, 1H), 8.22 (d, 1H, *J* = 7.8 Hz), 8.18 (d, 1H, *J* = 7.2 Hz), 8.05 (s, 1H), 7.68 (t, 1H, *J* = 7.8 Hz), 7.33 (m, 5H), 7.19 (m, 1H), 7.04 (m, 1H), 6.57 (d, 1H, *J* = 7.2 Hz), 4.99 (m, 1H), 1.94 (m, 2H), 0.96 (t, 1H, *J* = 7.2 Hz).

6.2.42. (E)-N-(2-Chlorobenzyl)-2-cyano-3-(5-(3-nitrophenyl)furan-2-yl)acrylamide (45)

¹H NMR (600 MHz, CDCl₃) δ 8.96 (t, 1H, *J* = 5.4 Hz), 8.72 (s, 1H), 8.31 (d, 1H, *J* = 6.0 Hz), 8.26 (d, 1H, *J* = 6.0 Hz), 8.09 (s, 1H), 7.84 (m, 1H), 7.65 (d, 1H, *J* = 3.6 Hz), 7.52 (d, 1H, *J* = 3.6 Hz), 7.46 (d, 1H, *J* = 7.8 Hz), 7.36 (m, 3H), 4.50 (s, 2H), 3.17 (d, 1H, *J* = 5.4 Hz).

6.2.43. (E)-2-Cyano-N-(4-methylbenzyl)-3-(5-(3-nitrophenyl)furan-2-yl)acrylamide (46)

¹H NMR (600 MHz, DMSO-*d*₆) δ 8.91 (t, 1H, *J* = 5.4 Hz), 8.71 (s, 1H), 8.30 (d, 1H, *J* = 7.8 Hz), 8.25 (d, 1H, *J* = 7.8 Hz), 8.06 (s, 1H), 7.84 (t, 1H, *J* = 6.0 Hz), 7.63 (d, 1H, *J* = 3.6 Hz), 7.49 (d, 1H, *J* = 3.6 Hz), 7.20 (d, 2H, *J* = 7.8 Hz), 7.14 (d, 2H, *J* = 7.8 Hz), 4.37 (d, 1H, *J* = 5.4 Hz), 3.17 (d, 1H, *J* = 4.8 Hz), 2.28 (s, 3H).

6.2.44. (E)-2-Cyano-N-(3-methoxybenzyl)-3-(5-(3-nitrophenyl)furan-2-yl)acrylamide (47)

¹H NMR (600 MHz, DMSO-*d*₆) δ 8.94 (t, 1H, *J* = 5.4 Hz), 8.72 (s, 1H), 8.31 (d, 1H, *J* = 7.8 Hz), 8.25 (d, 1H, *J* = 7.8 Hz), 8.07 (s, 1H), 7.84 (t, 1H, *J* = 7.8 Hz), 7.63 (d, 1H, *J* = 3.6 Hz), 7.50 (d, 1H, *J* = 3.6 Hz), 7.26 (t, 1H, *J* = 7.8 Hz), 6.89 (s, 2H), 6.83 (d, 1H, *J* = 6.0 Hz), 4.40 (d, 1H, *J* = 6.0 Hz), 3.75 (s, 3H).

6.2.45. (E)-2-Cyano-N-((5-methylfuran-2-yl)methyl)-3-(5-(3-nitrophenyl)furan-2-yl)acrylamide (48)

¹H NMR (600 MHz, DMSO-*d*₆) δ 8.85 (t, 1H, *J* = 5.4 Hz), 8.71 (s, 1H), 8.30 (d, 1H, *J* = 8.4 Hz), 8.25 (d, 1H, *J* = 8.4 Hz), 8.05 (s, 1H), 7.84 (t, 1H, *J* = 7.8 Hz), 7.64 (d, 1H, *J* = 3.6 Hz), 7.49 (d, 1H, 3.6 Hz), 2.24 (s, 3H), 6.16 (s, 1H), 6.00 (s, 1H), 4.35 (d, 2H, *J* = 5.4 Hz).

6.3. General procedure for reductive amination using asymmetric aromatic amines with BAL-PG-PS resin

Resin (1 g), NaBH₃CN (1.56 g, 25 equiv), DCE (35 mL) 2-phenyl ethyl amine (3.25 mL, 25 equiv), AcOH (0.38 mL, 4 equiv) was rotated on orbital shaker for 24 h. The resultant secondary amine resin was washed with DCM (10 mL × 10) and DMF-CH₂Cl₂ (1:1) (10 mL × 10) and dried well. The reaction was checked by the ninhydrin test (color shows purple).

6.4. General procedure for cyanoacylation of secondary amine

A solution of cyanoacetic acid (3 g, 20 equiv), DIPCDI (20 equiv), DIPEA (20 equiv) in DMF (30 mL) was added to the above resin and rotated on an orbital shaker for 7 h. The resin was washed with DMF (20 mL × 10) and the acylation was repeated for another 7 h. The resin was washed and dried. The reaction was checked by ninhydrin test.

6.5. General procedure for Knoevenagel condensation

A solution of aldehyde (5 equiv) in anhydrous DMF/EtOH (10:2) (1.5 mL) and 10 drops of piperidine was added to the above resin in 96 wells and shaken over night. The reaction mixture was drained, and the resin was washed with DMF (1.5 mL × 10).

6.6. General procedure for final cleavage

All products were cleaved from the resin with 90% TFA in water for 1.5 h and collected from 96-well deep well blocks. The solvent was removed in vacuo washed three times with ether and the residues were dissolved in CH₃CN and analyzed by LC/MS.

6.7. Preparation of degrasyn using solid support lanterns**6.7.1. General procedure for reductive amination**

A-series BAL Lantern (initial specified loading: 750 μmol) is treated with 11 mL of a solution of amine (0.5 M, 5.3 mmol, 7-mol equiv) and sodium cyanoborohydride (0.05 M, 530 μmol, 0.7 mol equiv) in 1% acetic acid/DMF at 60 °C for 17 h. After cooling to rt, the reagent solution is decanted and the Lanterns washed with DMF (3 × 3 min) and DCM (3 × 3 min) 20 mL.

6.7.2. General procedure for cyanoacylation of secondary amine
Same as resin.**6.7.3. General procedure for Knoevenagel condensation**
Same as resin.**6.7.4. General procedure for final cleavage**
Same as resin.**7. Molecular modeling****7.1. Ligand preparation**

Each of the compounds were drawn into ChemDraw, exported in MOL format, and concatenated into a single SDF formatted file.

LigPrep²¹ was used to generate a single 3D structure of each compound. A MacroModel²² conformational search using the mixed torsional/low-mode sampling method was used to generate five representative low energy starting configurations for the quantum chemical calculations. The OPLS2005 force field²³ was used with water solvent. The default value for the maximum iterations during minimization was increased from 500 to 1500 to allow for convergence that is more consistent. The number of steps for conformation search was increased to 1500 steps and redundant conformers were eliminated based on 1.0 Å RMSD cutoff. Additionally, the dihedral C=C–C(=O)–N between double bond and carbonyl was fixed at 180.0° to avoid a bias of sampling configuration near 0.0°, which was observed during the conformational search, but not observed as favorable during ab initio calculations.

7.2. Quantum chemical calculations

Quantum chemical calculations were completed using Jaguar (Version 7.6, Schrödinger, LLC, New York, NY, 2009). All geometry optimization were completed using Density Functional Theory (DFT) and B3LYP functional. As many structures contain a Br atom, it was necessary to select a basis set with an effective core potential (ECP). Both the LACVP and LACV3P basis sets utilizes the 6-31G basis set for all atoms H–Ar, and the LCA pseudopotential for Br.²⁴ Calculation on the five low-energy structures from conformational search were completed with the LACVP* basis set and the lowest configuration for each was submitted for full property analysis at with the LACV3P** level. Molecular orbital surfaces were created for the LUMO level in each case and these were mapped onto the electron density to highlight the preferred position of attack of HOMO of cysteine. The atomic Fukui indices²⁵ were also calculated for each structure to give a numeric measure of the reactivity. In particular, we focused on the LUMO f_{NN} value, which is a measure of the change in electron density when a molecule undergoes reaction with a change in electron density but spin density held constant. This quantity relates the reactivity of each atom towards an incoming nucleophile.²⁶ This value may also be combined with the global electrophilicity index ω , to give the atom electrophilicity index, ω_k via the equation, $\omega_k = f_{NN} \omega$.²⁷ The global electrophilicity index is a more absolute scale of electrophilicity that is independent of the nucleophilic partner. It is defined as $\omega = \mu^2/2\eta$; where $\mu \approx (\epsilon_H + \epsilon_L)/2$ and $\eta \approx \epsilon_L - \epsilon_H$.

8. Biology

8.1. Screening for anti-tumor activity

All compounds are tested for purity (HPLC, NMR) and the calculated molecular weight is used to make up a 10 mM stock solution of each compound (in 100% dimethylsulfoxide or 50% dimethylsulfoxide:50% polyethylene glycol 300). Compounds are diluted into cell culture media consisting of RPMI1640 with 10% fetal bovine serum to a final starting concentration of 10 μ M. [Highest final DMSO content = 0.1%]. Tumor cells (20,000) are plated into individual wells of a 96-well culture plate in 0.1 mL of culture media. Diluted compounds are added to individual wells containing pre-plated cells (final volume 0.2 mL) and incubated at 37 °C for 24–72 h. Well receive vehicle alone as a control.

8.2. MTT (viability) assay

MTT reagent (20 μ l of 5 mg/mL stock solution, Sigma) is added to the cells and the plates are incubated at 37 °C for another 2 h. Cells are lysed by adding 100 μ l of lysis buffer (20% SDS in 50% N,N-dimethylformamide (Sigma) adjusted to pH 4.7 by 80% acetic

acid and 1 M HCl such that the final concentration of acetic acid is 2.5% and HCl is 2.5%) into each well and incubated for 6 h. The OD₅₇₀ of each sample is determined by using a SPECTRA MAX M2 plate reader (Molecular Devices). The OD in control and treated wells is used as an estimate of the effect of compounds on cell growth and survival.

8.3. Cell lines

Multiple myeloma cell lines (MM-1, U266, OCI-My4) were grown in RPMI 1640 containing 10% heat-inactivated fetal bovine serum and 2 mM glutamine.

Acknowledgements

The authors thank Cancer Center support grant CA016672 for the support of the translational chemistry core Facility and NMR facility at M. D. Anderson Cancer Center. We also gratefully acknowledge funding support from Callisto Pharmaceuticals (New York, NY).

Supplementary data

Supplementary data associated with this article can be found, in the online version, at doi:10.1016/j.bmc.2011.09.057.

References and notes

- Meydan, N.; Grunberger, T.; Dadi, H.; Shahar, M.; Arpaia, E.; Lapidot, Z.; Leeder, J. S.; Freedman, M.; Cohen, A.; Gazit, A.; Levitzki, A.; Roifman, C. M. *Nature* **1996**, *379*, 645.
- Catlett-Falcone, R.; Landowski, T. H.; Oshiro, M. M.; Turkson, J.; Levitzki, A.; Savino, R.; Ciliberto, G.; Moscinski, L.; Fernandez-Luna, J. L.; Nunez, G.; Dalton, W. S.; Jove, R. *Immunity* **1999**, *10*, 105.
- Alas, S.; Bonavida, B. *Clin. Cancer Res.* **2003**, *9*, 316.
- Burdelya, L.; Catlett-Falcone, R.; Levitzki, A.; Cheng, F.; Mora, L. B.; Sotomayor, E.; Coppola, D.; Sun, J.; Sebt, S.; Dalton, W. S.; Jove, R.; Yu, H. *Mol. Cancer Ther.* **2002**, *1*, 893.
- Bharti, A. C.; Donato, N.; Aggarwal, B. B. *J. Immunol.* **2003**, *171*, 3863.
- Verma, A.; Kambhampati, S.; Parmar, S.; Platanius, L. C. *Cancer Metastasis Rev.* **2003**, *22*, 423.
- Kerr, I. M.; Costa-Pereira, A. P.; Lillemeier, B. F.; Strobl, B. *FEBS Lett.* **2003**, *546*, 1.
- Levitzki, A.; Gazit, A.; Roifman, C. *PCT Int. Appl.* (1995), WO 9528922 A1 19951102, 1995, 35 pp.
- Gu, L. *PCT Int. Appl.* (2003), WO 2003068157 A2 20030821, 2003, 38 pp.
- Priebe, W.; Donato, N.; Talpaz, M.; Szymanski, S.; Fokt, I.; Levitki, A. *PCT Int. Appl.* (2005), WO 2005058829 A1 20050630, 2005, 56 pp.
- Constantin, G.; Brocke, S.; Izikson, A.; Laudanna, C.; Butcher, E. C. *Eur. J. Immunol.* **1998**, *28*, 3523.
- Iwamaru, A.; Szymanski, S.; Iwado, E.; Aoki, H.; Yokoyama, T.; Fokt, I.; Hess, K.; Conrad, C.; Madden, T.; Sawaya, R.; Kondo, S.; Priebe, W.; Kondo, Y. *Oncogene* **2007**, *26*, 2435.
- Iwamaru, A.; Szymanski, S.; Iwado, E.; Aoki, H.; Yokoyama, T.; Fokt, I.; Hess, K.; Conrad, C.; Madden, T.; Sawaya, R.; Kondo, S.; Priebe, W.; Kondo, Y. *Oncogene* **2007**, *26*, 2435.
- Bartholomeusz, G. A.; Talpaz, M.; Kapuria, V.; Kong, L. Y.; Wang, S.; Estrov, Z.; Priebe, W.; Wu, J.; Donato, N. *J. Blood* **2007**, *109*, 3470.
- Demin, P.; Rounova, O.; Grunberger, T.; Cimpean, L.; Sharfe, N.; Roifman, C. M. *Bioorg. Med. Chem.* **2004**, *12*, 3019.
- Sun, H.; Kapuria, V.; Peterson, L. F.; Fang, D.; Bornmann, W. G.; Bartholomeusz, G.; Talpaz, M.; Donato, N. *J. Blood* **2011**, *117*, 3151.
- Kapuria, V.; Peterson, L. F.; Fang, D.; Bornmann, W. G.; Talpaz, M.; Donato, N. *J. Cancer Res.* **2010**, *70*, 9265.
- Gazit, A.; Oshero, N.; Posner, I.; Yaish, P.; Poradosu, E.; Gilon, C.; Levitzki, A. *J. Med. Chem.* **1991**, *34*, 1896.
- Gu, L.; Zhuang, H.; Safina, B.; Xiao, X. Y.; Bradford, W. W.; Rich, B. E. *Bioorg. Med. Chem.* **2005**, *13*, 4269.
- Shi, S.; Xiao, X. Y.; Czarnik, A. W. *Biotechnol. Bioeng.* **1998**, *61*, 7.
- LigPrep, Version 2.3; Schrödinger, LLC, New York, NY, 2009.
- MacroModel, Version 9.7; Schrödinger, LLC, New York, NY, 2009.
- Kaminski, G. A.; Friesner, R. A.; Tirado-Rives, J.; Jorgensen, W. L. *J. Phys. Chem. B* **2001**, *105*, 6474.
- Hay, P. J.; Wadt, W. R. *J. Chem. Phys.* **1985**, *82*, 299.
- Chamorro, E.; Perez, P. *J. Chem. Phys.* **2005**, *123*, 114107.
- Mondal, P.; Hazarika, K. K.; Deka, R. C. *PhysChemComm* **2003**, *24*.
- Domingo, L. R.; Perez, P.; Contreras, R. *Tetrahedron* **2004**, *60*, 6585.